

Figure 5. Far-infrared spectra (600–200 cm^{-1}) of $\text{Rh}_2(\text{CH}_3\text{COS})_4\text{L}_2$ as wax disks at room temperature with (a) $\text{L} = \text{PPh}_3$, (b) $\text{L} = \text{AsPh}_3$, and (c) $\text{L} = \text{SbPh}_3$.

V. The appearance of an overtone and combination tone involving $\nu_1(\text{RhRh})$ in the Raman spectra taken at resonance with the ca. 400-nm band supports the earlier assignment of this electronic transition to $\sigma(\text{RhRh}) \rightarrow \sigma^*(\text{RhRh})$, since the Rh–Rh bond length in the σ^* state would be expected to be longer than in the ground state. However, the appearance of an overtone of $\nu_2(\text{Rh-bridge})$ suggests that the resonant transition may have some Rh–bridge character to it as well. Moreover, the lack of long progressions in ν_1 at resonance with the $\sigma \rightarrow \sigma^*$ transition (such as are typical of the resonance Raman spectra of the analogous tetraacetate complexes) indicates that excitation leads to small geometric changes along several coordinates rather than to a more substantial

change essentially along the ν_1 coordinate alone.¹⁹

Infrared Spectra. Far-infrared spectra of $\text{Rh}_2(\text{CH}_3\text{COS})_4\cdot 2\text{L}$ ($\text{L} = \text{PPh}_3, \text{AsPh}_3, \text{SbPh}_3$) are shown in Figure 5, and the bands have been listed in Table VI along with their assignments. Three bands at 279, 316, and 550 cm^{-1} in each spectrum shift very little on changing L, and these have been assigned to infrared-active $\nu(\text{Rh-S}), \nu(\text{Rh-O})$, and $\delta(\text{OCS})$ modes of the $\text{Rh}_2(\text{CH}_3\text{COS})_4$ skeleton by comparison with assignments for analogous compounds.^{11,18} Strong bands at 496, 502, and 514 cm^{-1} , with $\text{L} = \text{PPh}_3$, do show a dependence on axial ligand, shifting to 472 cm^{-1} with $\text{L} = \text{AsPh}_3$ and 450 cm^{-1} with $\text{L} = \text{SbPh}_3$. These are assigned to $\gamma\text{-X-sens}$ and $t\text{-X-sens}$ modes (Whiffen's nomenclature^{16,17}) of the axial ligands by analogy with previous assignments of bands observed at similar wavenumbers in the spectra of $\text{Rh}_2(\text{CH}_3\text{CO}_2)_4\cdot 2\text{L}$ ($\text{L} = \text{PPh}_3, \text{AsPh}_3, \text{SbPh}_3$).¹⁻³

Intense bands attributable to skeletal $\nu(\text{C-S})$ and $\nu(\text{C-O})$ modes appear at 703 and 1545 cm^{-1} with $\text{L} = \text{PPh}_3$, 697 and 1548 cm^{-1} with $\text{L} = \text{AsPh}_3$, and 698 and 1544 cm^{-1} with $\text{L} = \text{SbPh}_3$. These have been assigned by comparison with literature infrared spectra of analogous compounds.¹⁸

Conclusion

The electronic and resonance Raman spectra of the complexes studied are fully consistent with the evidence from X-ray crystallographic studies that the Rh–Rh bond distance in dirhodium tetrakis(thiocarboxylates) is considerably longer than in dirhodium tetracarboxylates. The strong band in the blue region of the visible spectrum of the tetrakis(thioacetates) is assigned to the $\sigma(\text{Rh})_2 \rightarrow \sigma^*(\text{Rh})_2$ transition; it exhibits a bathochromic shift of ca. 2000–4000 cm^{-1} relative to that found for the analogous dirhodium tetraacetate, this being indicative of a weaker, longer $\sigma(\text{Rh})_2$ bond for the former. The most intense band in the Raman and resonance Raman spectra of $\text{Rh}_2(\text{CH}_3\text{COS})_4\cdot 2\text{L}$ ($\text{L} = \text{PPh}_3, \text{AsPh}_3, \text{SbPh}_3$) is assigned to $\nu_1(\text{RhRh})$ at 226–242 cm^{-1} . It occurs at an appreciably lower wavenumber than $\nu_1(\text{RhRh})$ of $\text{Rh}_2(\text{CH}_3\text{CO}_2)_4\cdot 2\text{L}$ ($\text{L} = \text{PPh}_3, \text{AsPh}_3, \text{SbPh}_3$) (289–307 cm^{-1}), and this is also in keeping with a weaker, longer Rh–Rh bond in tetrakis(thioacetates) than in tetraacetates.

Acknowledgment. We are grateful to the Wolfson Foundation for a grant (to support R.W.) and to the ULIRS for support.

(18) Kireeva, I. K.; Mazo, G. Ya.; Shchelokov, R. N. *Russian Inorg. J. Chem.* 1979, 24, 220.

(19) Clark, R. J. H.; Dines, T. J. *Angew. Chem., Int. Ed. Engl.* 1986, 25, 131.

Contribution from the Departments of Chemistry, College of General Education, Nagoya University, Chikusa-ku, Nagoya 464-01, Japan, College of General Education, Osaka University, Toyonaka, 560 Japan, and Daido Institute of Technology, Minami-ku, Nagoya, 457 Japan

XANES Spectra of Copper(II) Complexes: Correlation of the Intensity of the $1s \rightarrow 3d$ Transition and the Shape of the Complex

Mitsuru Sano,^{*,†} Seiko Komorita,[‡] and Hideo Yamatera[§]

Received July 6, 1990

X-ray absorption spectra are measured for several copper complexes with four identical ligands, $[\text{CuL}_4]^{2-}$ ($\text{L} = \text{chloro, succinimidato}$), whose geometry ranges from tetrahedral to square planar. Although the main features change complicatedly, the intensity of the $1s \rightarrow 3d$ peak increases with the increase in the dihedral angle between the two L-Cu-L planes. The relation between the intensity and the dihedral angle is explained by correlating the intensity with the mixing of the Cu 3d and 4p orbitals through the perturbation of the ligand field.

Introduction

XANES gives information complementary to that extracted from EXAFS concerning the coordination geometry and electronic structure an absorbing atom; this is particularly important in the

study of systems for which EXAFS is of limited usefulness.¹ Although X-ray absorption spectra near K-edge have been reported for many years, the relations between the spectral characteristics such as the intensity, shape, and location of edge features and the ligand field geometry and electronic structure of the absorbing atom still remain to be addressed in further systematic

[†]Nagoya University.

[‡]Osaka University.

[§]Daido Institute of Technology.

(1) Bianconi, A.; Garofa, J.; Benfatto, M. *Top. Current Chem.* 1988, 145, 29.

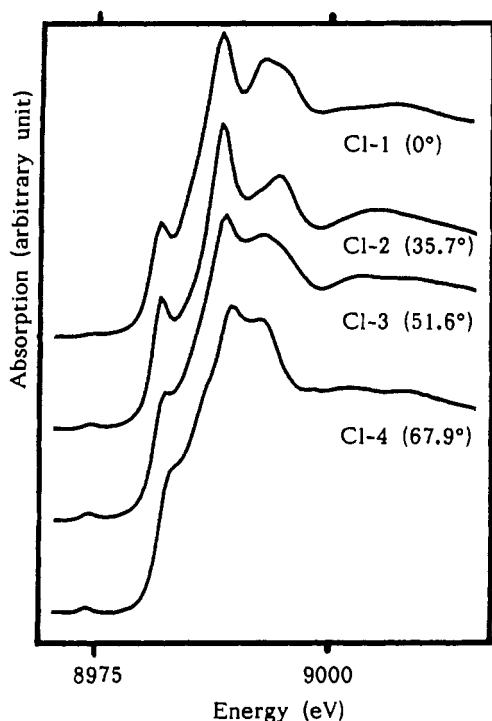


Figure 1. Cu K-edge spectra of $[\text{CuCl}_4]^{2-}$ (CI-1 = $[(\text{C}_6\text{H}_5)_2\text{CH}_2\text{CH}_2\text{N}-\text{H}_2\text{CH}_3]_2\text{CuCl}_4$, CI-2 = $[\text{Pt}(\text{en})_2\text{Cl}_2]\text{CuCl}_4$, CI-3 = $(N\text{-phenyl-piperazinium})_2\text{CuCl}_4$, CI-4 = Cs_2CuCl_4). In parentheses are given the dihedral angles between the two Cl-Cu-Cl planes.

studies. Roe et al.² reported iron K-edge absorption features and showed a good correlation of $1s \rightarrow 3d$ transition intensity with coordination number for iron compounds and also with the total percentage of Fe 4p atomic orbitals in the mainly 3d molecular orbital. Kau et al.³ studied the XANES of the copper complexes and found the relation between the coordination number of the complex and its XANES. We hope to establish further experimental XANES rules, which provide us with a powerful tool for the determination of the local structure of complex systems like proteins, surfaces, and amorphous materials.

Copper(II) ions have been extensively investigated for the great ease with which they assume various geometries. Thus, a copper(II) complex is one of the best compounds to investigate to determine the correlation between edge features and the ligand field geometry. We recorded Cu K-XANES spectra of several four-coordinate copper(II) compounds with ligand field geometries ranging from tetrahedral to square planar and studied the relation between the XANES features and the dihedral angle of the two ligand-copper-ligand planes. The results were explained by an angular overlap approach.

Experimental Section

The copper complexes were prepared according to standard methods.⁴⁻⁸ Samples were ground and diluted with boron nitride and contained in a plastic cell. X-ray absorption measurements were carried out at the BL-10B on the storage ring of the Photon Factory at the National Laboratory of High Energy Physics (KEK). Synchrotron radiation (2.5 GeV, 120–280 mA) was monochromatized with a channel-cut Si(311) monochromator.^{9,10} The absorption spectra were measured in the

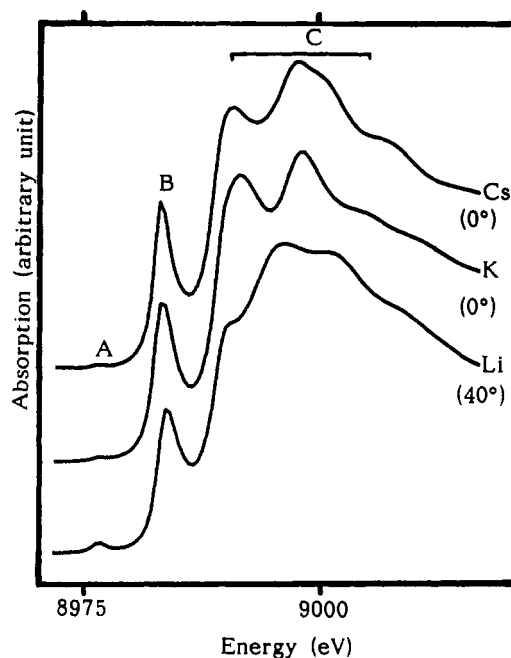


Figure 2. Cu K-edge spectra of $[\text{Cu}(\text{succd})_4]^{2-}$ (Cs = $\text{Cs}_2[\text{Cu}(\text{succd})_4]$, K = $\text{K}_2[\text{Cu}(\text{succd})_4]$, Li = $\text{Li}_2[\text{Cu}(\text{succd})_4] \cdot \text{H}_2\text{O}$).

Table I. Correlation of the $1s \rightarrow 3d$ Intensity with the Dihedral Angle between the Ligand-Cu-Ligand Planes

compd ^a	dihedral angle, deg	$1s \rightarrow 3d$ peak height
Cu(imidazole) ₄ SO ₄	0	0.010 ± 0.003
CuSO ₄ ·5H ₂ O	0	0.013 ± 0.003
CI-1	0	0.009 ± 0.003
CI-2	35.7	0.018 ± 0.003
CI-3	51.6	0.022 ± 0.003
CI-4	67.9	0.023 ± 0.003
Cs	0	0.012 ± 0.003
K	0	0.013 ± 0.003
Li	40.0	0.036 ± 0.003

^a For abbreviations, see the captions to Figures 1 and 2.

transmission mode at room temperature. The incident- and transmitted-beam intensities were measured with N₂- and Ar(15%)-N₂-filled ionization chambers, respectively.¹⁰ All spectra have been normalized to give an edge jump of 1.0.

Results and Discussion

Four Cu XANES spectra of $[\text{CuCl}_4]^{2-}$ are shown in Figure 1. The features change with the dihedral angle at the copper atom. According to previous studies,^{11,12} this noticeable change is not due to counterions but to the ligand field geometry, which shows that XANES is sensitive to the environment around the absorbing atom. All the compounds show a weak pre-edge peak and a shoulder; with increasing dihedral angle,⁴⁻⁸ the pre-edge peak remains almost unchanged at about 8974 eV in energy and increases in its intensity. Although the assignment of the main absorption peaks consisting of three or more transitions differs between authors,¹³⁻¹⁵ the weak pre-edge peak is definitely assigned to the $1s \rightarrow 3d$ transition.

- Roe, A. L.; Schneider, D. J.; Mayer, R. J.; Widom, J.; Que, L., Jr. *J. Am. Chem. Soc.* **1984**, *106*, 1676.
- Kau, L.; Spira-Solomon, D. J.; Penner-Hahn, J. E.; Hodgson, K. O.; Solomon, E. I. *J. Am. Chem. Soc.* **1987**, *109*, 6433.
- Yamada, S.; Miki, S. *Bull. Chem. Soc. Jpn.* **1963**, *36*, 680.
- McGinney, J. A. *J. Am. Chem. Soc.* **1972**, *94*, 8406.
- Battaglia, L. P.; Corradi, A. B.; Marrotrigiano, G.; Menabue, L.; Pellacani, G. C. *Inorg. Chem.* **1979**, *18*, 148.
- Larsen, K. P.; Hazell, R. G.; Toftlund, H.; Andersen, P. R.; Bisgard, P.; Edlund, K.; Eliassen, M.; Herskind, C.; Laursen, T.; Pedersen, P. M. *Acta Chem. Scand., Ser. A* **1975**, *29*, 499.
- Harlow, R. L.; Wells, W. J.; Watt, G. W.; Simonsen, S. H. *Inorg. Chem.* **1974**, *13*, 2106.

- Oyanagi, H.; Matsushita, T.; Ito, M.; Kuroda, H. *KEK Rep.* **1983**, No. 83-10.
- Nomura, M. *KEK Rep.* **1987**, No. 87-1 (and private communication). Energy resolution is less than 1 eV at 9 keV for this spectrum, and harmonic contamination is negligible under these experimental conditions. The energy was calibrated with respect to the first inflection point of the Cu metal absorption edge, defined to be 8978.8 eV.
- Sano, M. *Chem. Phys. Lett.* **1988**, *148*, 331.
- Sano, M. *Inorg. Chem.* **1988**, *27*, 4249.
- Bair, R. A.; Goddard, W. A. III. *Phys. Rev.* **1980**, *B22*, 2767.
- Kosugi, N.; Yokoyama, T.; Asakura, K.; Kuroda, H. *Chem. Phys.* **1984**, *91*, 249. Kosugi, N.; Kondoh, H.; Tajima, H.; Kuroda, H. *Physica B (Amsterdam)* **1989**, *158*, 450.
- Smith, T. A.; Penner-Hahn, J. E.; Berding, M. A.; Doniach, S.; Hodgson, K. O. *J. Am. Chem. Soc.* **1985**, *107*, 5945.

Figure 2 shows XANES spectra of $[\text{Cu}(\text{succd})_4]^{2-}$ (succd = succinimidate ion). The spectra of two square-planar chromophores¹⁶ are similar to each other but different from that of a compressed tetrahedral (D_{2d}) one.¹⁷ This also shows that XANES spectra are very sensitive to the ligand field geometry. The energy of absorption B increases in going from D_{4h} to D_{2d} geometry. The same tendency is also shown by the corresponding peak of the spectra of chloride complexes, in which the peak is overlapped by an intense peak and is made less pronounced. The behavior of absorption band C is complicated.

Table I shows the dihedral angle of the two ligand-copper-ligand planes of each complex and the intensity of the $1s \rightarrow 3d$ peak.¹⁸ The intensity is low for planar complexes and increases with increasing dihedral angle for complexes of the same chemical composition. This empirical relation provides a basis for estimating the dihedral angle from the $1s \rightarrow 3d$ intensity.

Theoretical Considerations

Now, we shall theoretically elucidate the experimental results. Although the $1s \rightarrow 3d$ transition is a g-g transition which is forbidden as an electric dipole transition, this transition may have nonzero intensity for the following reasons: (1) a magnetic dipole transition and an electric quadrupole transition, which are weak but are allowed, (2) a vibronic coupling with odd-parity molecular vibrations related to the Cu-Cl bond, (3) mixing of Cu 3d and ligand orbitals, and (4) mixing of Cu 3d and 4p orbitals (4a) due to disorder in Cu-Cl distances or (4b) due to perturbation of a D_{2d} ligand field. As will be verified by the following discussion, reason 4b is most important in the present case.

Reason 1 is not important for the matter of present concern, because the intensity of an allowed transition (magnetic dipole or electric quadrupole) will not be significantly influenced by the environment. We acknowledge the unambiguous experimental finding of Hahn et al.¹⁹ that the $1s \rightarrow 3d$ transition in square-planar $[\text{CuCl}_4]^{2-}$ is primarily due to an electric quadrupole transition. This is also confirmed by our rough estimate of the intensity ratio²⁰

$$\frac{1s \rightarrow 3d \text{ electric quadrupole transition}}{1s \rightarrow 4p \text{ electric dipole transition}} = 5.7 \times 10^{-4} \quad (1)$$

However, in tetrahedral complexes, where the $1s \rightarrow 3d$ peak was found to be 2-3 times as high as that in a square-planar complex, the electric quadrupole transition is responsible for only a minor part of the intensity.

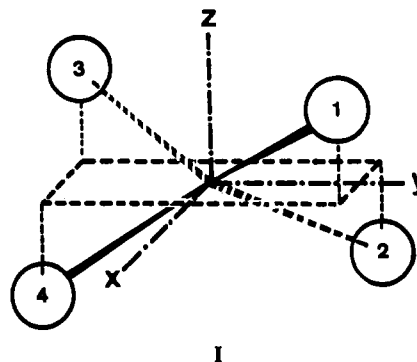
Vibronic coupling (reason 2) is well-known to play an important role in UV-visible absorption spectra of transition-metal complexes. Hahn et al.¹⁹ attributed one-third of the $1s \rightarrow 3d$ intensity in square-planar $[\text{CuCl}_4]^{2-}$ to the dipole contribution from vibronic

coupling. We agree that vibronic coupling is partly responsible for the intensity. However, there is no reason that the vibronic coupling should be much more effective in tetrahedral complexes than in a square-planar one.

According to McDonald et al.,²¹ the mixing of the Cu 3d orbital with the ligand orbital has a significant effect on the intensity of d-d transitions. However, the overlap integral between the Cu 1s and the ligand orbitals is practically zero, so that $1s \rightarrow 3d$ transitions cannot borrow intensity from allowed transitions in which ligand orbitals are involved. Thus reason 3 can be eliminated in the present case.

Next, we consider the disorder in Cu-Cl distances (reason 4a). Although crystal analyses⁴⁻⁸ show slight variations in Cu-Cl distances of $[\text{CuCl}_4]^{2-}$, no clear correlation is found between the disorder and the $1s \rightarrow 3d$ intensity. Therefore, reason 4a does not seem essential to our consideration of the $1s \rightarrow 3d$ intensity.

Now, we shall consider the mixing of the 3d and 4p orbitals through the perturbation of the ligands (reason 4b). In a coordinate system as shown in I, the hole in the 3d shell of Cu^{2+} exists



in the d_{xy} orbital, which can mix with a ligand group orbital, ψ_L^0 , both orbitals belonging to the B_2 representation of the point group D_{2d} .

$$\psi_L^0 = \frac{1}{2}(\psi_1 - \psi_2 + \psi_3 - \psi_4)$$

The $4p_x$ orbital, which also belongs to B_2 , can mix with ψ_L^0 . Although $3d_{xy}$ (ψ_d^0) and $4p_x$ (ψ_p^0) do not directly mix with each other, ψ_d^0 is perturbed by the ligand field component of the B_2 symmetry, resulting in a perturbed $3d_{xy}$ orbital, ψ_d (to the second order):

$$\psi_d = \psi_d^0 + \left[\frac{H_{dL}^{(1)}}{E_d^0 - E_L^0} - \frac{H_{dd}^{(1)}H_{dL}^{(1)}}{(E_d^0 - E_L^0)^2} \right] \psi_L^0 + \left[\frac{H_{pL}^{(1)}H_{dL}^{(1)}}{(E_d^0 - E_p^0)(E_d^0 - E_L^0)} \right] \psi_p^0 \quad (2)$$

Here $H_{ij}^{(1)}$'s represent matrix elements of the perturbation $H^{(1)}$ and E_i^0 's the energies of the unperturbed i orbitals; terms containing $H_{pd}^{(1)}$ ($=0$) are omitted.

While the transition $\psi_{1s} \rightarrow \psi_d^0$ is forbidden, $\psi_{1s} \rightarrow \psi_L^0$ and $\psi_{1s} \rightarrow \psi_p^0$ are allowed; the $\psi_{1s} \rightarrow \psi_L^0$ transition, however, has practically zero probability, because the ligand orbitals hardly overlap with the 1s orbital. Thus, only the last term of eq 2 contributes to the transition probability; i.e., the intensity of the $1s \rightarrow 3d$ transition is proportional to the square of the coefficient of ψ_p^0 in eq 2. The denominator of this coefficient is approximately the same for all $[\text{CuCl}_4]^{2-}$ complexes under consideration. Thus, the relative intensity depends primarily on the magnitude of the numerator $H_{pL}^{(1)}H_{dL}^{(1)}$. Each of these matrix elements of perturbation can be expressed as a product of the radial and the angular parts:

$$H_{pL}^{(1)} \equiv \langle \psi_p^0 | H^{(1)} | \psi_L^0 \rangle = \langle \psi_p^0 | H^{(1)} | \psi_L^0 \rangle_{\text{rad}} \langle \psi_p^0 | \psi_L^0 \rangle_{\text{ang}}$$

$$H_{dL}^{(1)} \equiv \langle \psi_d^0 | H^{(1)} | \psi_L^0 \rangle = \langle \psi_d^0 | H^{(1)} | \psi_L^0 \rangle_{\text{rad}} \langle \psi_d^0 | \psi_L^0 \rangle_{\text{ang}}$$

(21) McDonald, R. G.; Riley, M. J.; Hitchman, A. *Inorg. Chem.* 1988, 27, 894.

(16) Tsukihara, T.; Katsube, Y.; Fujimori, K.; Kawashima, K.; Kannan, Y. *Bull. Chem. Soc. Jpn.* 1974, 47, 1582.

(17) Tsukihara, T.; Katsube, Y.; Fujimori, K.; Ito, T. *Bull. Chem. Soc. Jpn.* 1972, 45, 2959.

(18) The intensity as a ratio of $1s \rightarrow 3d$ peak height to Cu K-edge absorption intensity was obtained by the following procedure: (1) background was subtracted by a fitting polynomial function (Victoreen function); (2) the Cu K-edge absorption was estimated as a cubic spline function fitting to the EXAFS region, and its intensity was calculated by the extrapolation of the estimated function at the pre-edge peak; (3) the $1s \rightarrow 3d$ intensity was evaluated as a ratio of the $1s \rightarrow 3d$ peak height and the estimated Cu K-edge intensity at the pre-edge peak position.

(19) Hahn, J. E.; Scott, R. A.; Hodgson, K. O.; Doniach, S.; Desjardins, S. R.; Solomon, E. I. *Chem. Phys. Lett.* 1982, 88, 595.

(20) Hydrogen-like wave functions with effective quantum numbers and effective nuclear charges derived from the Slater rule were used in the calculation: 1 and 28.7 for 1s, 3 and 8.85 for 3d, and 3.7 and 5.55 for 4s, respectively. The ratio of the experimental peak height of the $1s \rightarrow 3d$ transition to that of the highest peak of the strong transitions at the edge (assigned to $1s \rightarrow 4p$ transitions by many investigators^{13,14}) is 0.009, or 0.007 after subtracting vibronic and other minor contributions (estimated to be one-third of the electric quadrupole transition, according to ref 19). Even the latter value is about 12 times as large as the calculated ratio; however, if the difference in the number of vacancies (1 for 3d but 2 for a nondegenerate 4p or 4 for degenerate 4p orbitals) and the difference in the observed bandwidth (the intense band is several times as wide as the $1s \rightarrow 3d$ band) are taken into account, the observed intensity ratio reasonably agrees with the calculated.

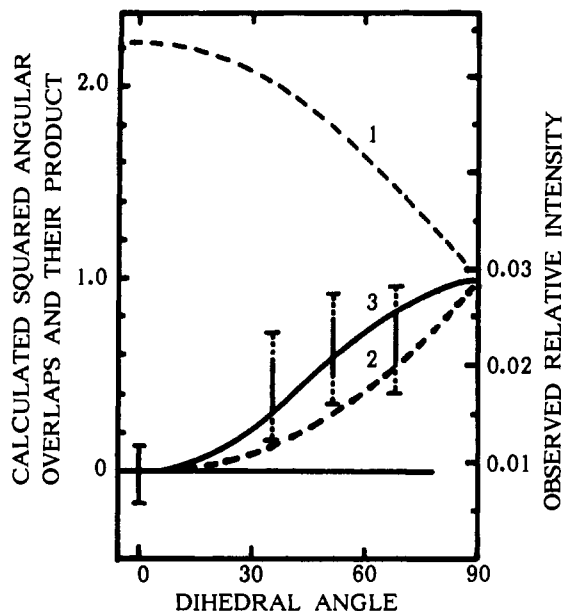


Figure 3. Relative magnitudes of squared angular overlap integrals and their product plotted against the dihedral angle between the Cl–Cu–Cl planes of $[\text{CuCl}_4]^{2-}$ and comparison of the calculated and observed intensities of the $1s \rightarrow 3d$ peak. Broken curve 1: $[(\psi_{p_z}^0|\psi_L^0)_{\text{ang}}]^2$ (normalized to 1.00 at 90°). Broken curve 2: $[(\psi_{p_x}^0|\psi_L^0)_{\text{ang}}]^2[(\psi_{p_y}^0|\psi_L^0)_{\text{ang}}]^2$ (normalized to 1.00 at 90°). Solid curve 3: $[(\psi_{d_{xy}}^0|\psi_L^0)_{\text{ang}}]^2[(\psi_{p_z}^0|\psi_L^0)_{\text{ang}}]^2$. Error bars: Experimental values. The dotted parts of the error bars show the error in setting the zero line for the calculated value, i.e., the error in the experimental value for the reference compound (the planar complex).

If the radial part of each matrix element is assumed to remain unchanged with the change in the dihedral angle (for complexes containing the same ligand with the same bond distance), the relative intensity of the $1s \rightarrow 3d$ transition will be proportional to the product of the squared angular overlap integrals: $[(\psi_{p_z}^0|\psi_L^0)_{\text{ang}}]^2[(\psi_{d_{xy}}^0|\psi_L^0)_{\text{ang}}]^2$. Although one observes a tendency for the Cu–Cl distances to decrease slightly with increasing dihedral angle, the change in the radial part can be expected to be much smaller than that in the angular part, in view of the general facts that the radial parameters of the angular overlap model (AOM) are transferable from one complex to another and that bond energies are also transferable from one compound to another.

Figure 3 shows the relative magnitudes of these squared angular overlap integrals and their product as a function of the dihedral angle between the Cl–Cu–Cl planes. For an easy comparison, both angular overlap integrals are normalized to unity at the dihedral angle of 90° . Figure 3 also shows a comparison of the theoretical prediction with the experimental results. If the intensity of the $1s \rightarrow 3d$ transition were solely due to the d–p mixing, the theory predicts that the transition probability would vanish for a planar complex. Actually in a planar complex, there occurs a very weak transition attributable to an electric quadrupole transition and an electric dipole contribution from vibronic coupling. To allow for these contributions which are expected to remain nearly the same with the change of the shape, the intensity observed for the planar complex was taken as the zero of the calculated (relative) intensity for a comparison between observed and calculated values. The intensity corresponding to the calculated zero could also be obtained by calculation (cf. eq 1 and ref 20). However, we have chosen the experimental value rather than the calculated one, because our calculation gives only a rough estimate. The calculated value, i.e., the product of two squared angular overlap integrals, shows a tendency similar to that of the observed $1s \rightarrow 3d$ intensities; both the observed and calculated intensities increase with increasing dihedral angle.

The results for succd complexes (Figure 2) showed the same trend as that observed for the chloro complexes; the $1s \rightarrow 3d$ intensity is low for planar complexes and much higher for the D_{2d} complex, although the intensity is higher for each succd complex than that for the chloro complex of a similar shape. The higher

intensities can be ascribed to the stronger Cu–succd bond or larger perturbation of the succd ligand field. A comparison of optical spectra suggests that the 3d orbitals are more strongly perturbed in the succd complexes than in the chloro complexes.²³ The XANES spectra, in which the features due to $1s \rightarrow 4p$ transitions appear at higher energies in the succd complexes, show that the 4p orbitals also undergo stronger perturbation in the succd complex. For a quantitative discussion, however, more experimental data and their full analyses will be needed.

Gewirth et al.²² have reported the values of charge distribution from an $X\alpha$ calculation of D_{2d} $[\text{CuCl}_4]^{2-}$, where the Cu sphere radius was adjusted to satisfy the observed g values. Their results show that the $5b_2$ ($d_{x^2-y^2}$) orbital, which corresponds to d_{xy} in the present coordinate system of D_{2d} , has 71% Cu character and 4% p character. This means the orbital has 3% Cu p character. The corresponding value from our XANES results is 1–2%, which is estimated as the peak height ratio (between 0.01 and 0.02, after subtracting the electric quadrupole and other minor contributions) times the bandwidth ratio (a few tenths) divided by the ratio of the number of vacancies ($1/4$ or $1/2$ for $3d$ /(degenerate $4p$) or $3d$ /(nondegenerate $4p$), respectively). Such a “slight” disagreement between the two values of the p character is allowable, because the XANES gives only a rough estimate and because the results of the $X\alpha$ calculation depend on adjustable parameters, which were optimized to fit to the g values, not the XANES results.

We also agree with Roe et al.² in correlating the area of the $1s \rightarrow 3d$ peak with the metal p character of the excited electron, although our estimate based on their experiments would give lower values of the p character.

Before concluding our discussion, it seems appropriate to mention the limitations and extensions of the present treatment. Since only the angular part of the wave functions is discussed here, the argument is limited to complexes of the same composition but of different shapes. However, the discussion will hopefully be extended to complexes with four identical ligand atoms and will be used as a clue in the qualitative determination of the structure of such four-coordinate complexes. Such an extended application can be expected, because it is known that the ligand field mainly depends on the ligating atom of the ligand.

Concluding Remarks

We have shown experimentally and theoretically that the intensity of the $1s \rightarrow 3d$ peak of the Cu XANES of $[\text{CuL}_4]$ -type complexes (with four identical ligands) can be correlated with the dihedral angle between the two L–Cu–L planes. The correlation is elucidated by an angular overlap approach.

The $1s \rightarrow 3d$ intensity is a useful parameter to investigate the local geometry around a metal ion in complicated systems such

(22) Gewirth, A. A.; Cohen, S. L.; Schugar, H. J.; Solomon, E. I. *Inorg. Chem.* **1987**, *26*, 1133.

(23) Komorita, S. Thesis, Osaka University, 1965. The peak of the ligand field band is located at a much higher wavenumber ($16\,100\text{ cm}^{-1}$) in $\text{Li}_2[\text{Cu}(\text{succd})_4] \cdot \text{H}_2\text{O}$ than in the chloro complexes ($12\,990\text{ cm}^{-1}$ in Cl-2, for example), indicating a much stronger ligand field in the succd complex. According to eq 2, the spectral intensity is proportional to the factor

$$[H_{pl}^{(1)}]^2[H_{dl}^{(1)}]^2 / [(E_d^0 - E_p^0)^2(E_d^0 - E_l^0)^2]$$

where $(E_d^0 - E_p^0)^2$ is a constant factor in the present approximation. The optical spectral data given above suggest that the value of $[H_{pl}^{(1)}]^2 / (E_d^0 - E_l^0)^2$ for the succd complex is about 1.3 times as large as that for the chloro complex after a minor correction for the difference in the dihedral angle. Although estimation of the remaining factor $[H_{dl}^{(1)}]^2 / (E_d^0 - E_l^0)^2$ is difficult, the fact that the shift of the intense ($1s \rightarrow 4p$) peaks relative to the $1s \rightarrow 3d$ peak is larger in the succd complex suggests that the $H_{pl}^{(1)}/H_{dl}^{(1)}$ ratio in the succd complex is larger than that in the chloro complex. If $H_{pl}^{(1)}/H_{dl}^{(1)}$ in the succd complex is assumed to be equal to that in the chloro complex, then the intensity of the $1s \rightarrow 3d$ peak in the succd complex will be 1.3² times as strong as that in the chloro complex, resulting in the relative intensity of $0.012 + (0.018 - 0.009) \times 1.7 = 0.027 (\pm 0.013)$. This value is the lower limit to be compared with the experimental value of $0.036 (\pm 0.003)$. The agreement is not so bad if it is considered that the calculated value is the lower limit and that processing of data accumulated experimental errors.

as metal-enzyme systems and catalysts, if the intensity is compared with those measured on appropriate reference compounds by using the same monochromator.

Acknowledgment. M.S. and H.Y. acknowledge Grants-in-Aid

No. 63740334 and No. 63540496 for Scientific Research from the Ministry of Education, Science, and Culture of Japan, respectively. This work has been performed under the approval of the Photon Factory Program Advisory Committee (Proposal No. 88-026).

Contribution from the Institut für Anorganische Chemie, LMU München, Meiserstrasse 1, D-8000 München 2, Germany, and Institut für Physikalische Chemie und Elektrochemie, Universität Karlsruhe, Kaiserstrasse 12, D-7500 Karlsruhe, Germany

Characterization of Matrix-Isolated Cu(CO)Cl. IR Spectroscopic Investigation and ab Initio Calculation

Harald S. Plitt,[†] Michael R. Bär,[‡] Reinhart Ahlrichs,^{*,‡} and Hansgeorg Schnöckel^{*,†}

Received May 22, 1991

Cocondensation of CuCl and CO in an argon matrix leads to new IR absorptions near 2157 and 362 cm⁻¹, which are assigned to a linear molecule Cl-Cu-CO. By means of large-scale ab initio calculations (CPF, MP2) the CuC distance is predicted to be 181 pm (CPF) and the reaction energy of CuCl + CO → ClCu-CO is reported to be 155 kJ mol⁻¹ exothermic (CPF). Bonding in this complex is discussed. The CuC bond is found to be formed by predominant σ -bonding from carbon to copper while $d\pi^*$ -back-donation from Cu to C plays a minor role.

Solutions of copper(I) chloride in hydrochloric acid are known to absorb CO.¹ Until recently, all attempts failed to isolate a well-defined solid containing CuCl and CO from these solutions or from similarly treated solutions of CuCl in organic solvents, e.g. THF or methanol.² In 1990, a simple preparation and structural characterization of solid Cu(CO)Cl was reported.³ In this solid, copper was found to be tetrahedrally coordinated by three chlorine atoms and the CO ligand. This type of bonding differs from that of gold in Au(CO)Cl, a molecule that has been shown to be linear in the solid state.⁴

The purpose of this paper is to describe our investigations on the products of the reaction of monomeric copper(I) chloride with CO in solid argon by means of IR spectroscopy and ab initio calculations. It is shown that experimental findings are in good agreement with data expected for a linear molecule Cu(CO)Cl.

Experimental Results

After cocondensation of monomeric CuCl⁵ and CO in an argon matrix,⁶ three additional absorptions at 2156.5, 361.6, and 356.1 cm⁻¹ arise. They cannot be observed in experiments performed with one of the reactants only. Using isotopically substituted CO, ¹³C¹⁶O and/or ¹²C¹⁸O, shifts in frequencies for these three bands have been detected as documented in Table I and Figure 1.

The absorptions in the CO region of the IR spectra only show isotopic shifts for ¹³C- and ¹⁸O-substitution; no chlorine or copper splitting can be observed. For this reason, the band at 2156.5 cm⁻¹ is assigned to a fairly uncoupled CO vibration (ν_{CO}) of the species under investigation. The absorptions at 361.6 and 356.1 cm⁻¹ exhibit an intensity pattern expected for a ³⁵Cl/³⁷Cl splitting.⁷ As these bands are also shifted by ¹³C- and ¹⁸O-substitution, they must be assigned to a highly coupled mode in the observed molecule, called $\nu_{ClCu/CuCO}$ in the following text.⁸ Even at very low concentrations of CuCl or CO in the matrix, the bands just described are detected. Thus, it is plausible to assign the observed absorptions to a species Cu(CO)Cl formed by reaction of monomeric CuCl with one molecule of CO.

Normal-Coordinate Analysis

In order to interpret the observed IR absorptions in terms of bond strengths, we performed a normal-coordinate analysis on the molecule Cu(CO)Cl with $C_{\infty v}$ symmetry. As all detectable frequencies belong to the irreducible representation Σ^+ , vibrations of this symmetry type have been considered only. We assume

Table I. IR Absorptions Assigned to Cu(CO)Cl (cm⁻¹)

	ν_{CO}	$\nu_{^{35}Cl-Cu-CO}$	$\nu_{^{37}Cl-Cu-CO}$
Cu(¹² C ¹⁶ O)Cl	2156.5	361.6	356.1
Cu(¹³ C ¹⁶ O)Cl	2107.4	358.7	353.9
Cu(¹² C ¹⁸ O)Cl	2107.8	355.8	350.0

Table II. Results of the Normal-Coordinate Analysis for Cu(CO)Cl^a

	$\Delta\nu_{CO}$	$\Delta\nu_{ClCu/CuCO}$	$\Delta\nu_{^{35}Cl/^{37}Cl}$
Cu(¹² C ¹⁶ O)Cl			5.53 (5.50)
Cu(¹³ C ¹⁶ O)Cl	49.98 (49.78)	2.66 (2.91)	5.42 (4.86)
Cu(¹² C ¹⁸ O)Cl	49.18 (49.30)	5.79 (5.82)	5.26 (5.83)

^a Force constants: $f_{CuCl} = 2.34$ mdyn/Å; $f_{CuC} = 2.35$ mdyn/Å; $f_{CO} = 18.59$ mdyn/Å; $f_{CuCl/CuC} = 0.1$ mdyn/Å; $f_{CuC/CO} = 0.5$ mdyn/Å; $f_{CuCl/CO} = 0.0$ mdyn/Å.

that there is no change in the CuCl bond during complexation; therefore, the force constant of uncoordinated monomeric CuCl⁹ has been inserted for f_{CuCl} in Cu(CO)Cl. The observed isotopic shifts have been corrected with respect to anharmonicity.¹⁰ Together with the calculated shifts, these values are collected in Table II, exhibiting good agreement with each other.

The force constant for the CuC bond ($f_{CuC} = 2.35$ mdyn/Å) is found to be of the magnitude of that for the CuCl bond ($f_{CuCl} = 2.34$ mdyn/Å) in monomeric CuCl. This value of f_{CuC} is low

- (1) Reviewed by: Bruce, M. I. *J. Organomet. Chem.* **1972**, *44*, 209 (with references up to 1970).
- (2) Pasquali, M.; Floriani, C.; Gaetani-Manfredotti, A. *Inorg. Chem.* **1981**, *20*, 3382.
- (3) Håkansson, M.; Jagner, S. *Inorg. Chem.* **1990**, *29*, 5241.
- (4) Jones, P. G. *Z. Naturforsch.* **1982**, *37B*, 823.
- (5) Monomeric copper(I) chloride has been prepared by reacting molecular chlorine with solid copper at 1000 °C in a Knudsen cell under vacuum conditions.
- (6) The matrix isolation equipment has been described previously: Ahlrichs, R.; Becherer, R.; Binnewies, M.; Borrmann, H.; Lakenbrink, M.; Schunck, S.; Schnöckel, H. *J. Am. Chem. Soc.* **1986**, *108*, 7905. All IR data have been collected using a Bruker IFS66v FT spectrometer ($\nu > 500$ cm⁻¹, resolution 1 cm⁻¹; $\nu < 500$ cm⁻¹, resolution 2 cm⁻¹).
- (7) According to the simple model of two vibrating masses, the absorption of a copper-chlorine vibration ($\nu \approx 360$ cm⁻¹) should exhibit a ³⁵/³⁷Cl splitting of about 6.3 cm⁻¹.
- (8) According to normal-coordinate analysis and ab initio calculations, the vibration $\nu_{ClCu/CuCO}$ corresponds to an in-phase motion of chlorine versus copper on one hand and of the CO group versus copper on the other hand.
- (9) Plitt, H. S.; Bär, M.; Ahlrichs, R.; Schnöckel, H. *Angew. Chem.* **1991**, *103*, 848; *Angew. Chem., Int. Ed. Engl.* **1991**, *30*, 832.
- (10) Becher, H. *J. Fortschr. Chem. Forsch.* **1968**, *10*, 156.

[†]LMU München.

[‡]Universität Karlsruhe.